Cell

The F-BAR Domain of srGAP2 Induces Membrane Protrusions Required for Neuronal Migration and Morphogenesis

Sabrice Guerrier,[1,2] Jaeda Coutinho-Budd,[3] Takayuki Sassa,[2] Aurélie Gresset,[1] Nicole Vincent Jordan,[1] Keng Chen,[4] Wei-Lin Jin,[4] Adam Frost,[5,6] and Franck Polleux[1,2,*]

[1]Department of Pharmacology, School of Medicine
[2]Neuroscience Research Center
[3]Neurobiology Curriculum
University of North Carolina at Chapel Hill, Chapel Hill, NC 27599, USA
[4]Institute of Neurosciences, Shanghai Jiao Tong University, Shanghai 200240, China
[5]Department of Molecular Biophysics and Biochemistry, Interdepartmental Neuroscience Program, Yale University School of Medicine, New Haven, CT 06510, USA
[6]Present address: Department of Cellular and Molecular Pharmacology and California Institute for Quantitative Biosciences, University of California, San Francisco, San Francisco, CA 94158, USA
*Correspondence: polleux@med.unc.edu
DOI 10.1016/j.cell.2009.06.047

SUMMARY

During brain development, proper neuronal migration and morphogenesis is critical for the establishment of functional neural circuits. Here we report that srGAP2 negatively regulates neuronal migration and induces neurite outgrowth and branching through the ability of its F-BAR domain to induce filopodia-like membrane protrusions resembling those induced by I-BAR domains in vivo and in vitro. Previous work has suggested that in nonneuronal cells filopodia dynamics decrease the rate of cell migration and the persistence of leading edge protrusions. srGAP2 knockdown reduces leading process branching and increases the rate of neuronal migration in vivo. Overexpression of srGAP2 or its F-BAR domain has the opposite effects, increasing leading process branching and decreasing migration. These results suggest that F-BAR domains are functionally diverse and highlight the functional importance of proteins directly regulating membrane deformation for proper neuronal migration and morphogenesis.

INTRODUCTION

During brain development, neural progenitor proliferation, neuronal migration, and differentiation require considerable changes in cell shape involving coordinated cytoskeletal and membrane remodeling (Ayala et al., 2007; Luo, 2002). Neuronal migration involves the coordinated extension and adhesion of the leading process (LP) along the radial glial scaffold with the forward translocation of the nucleus, which requires regulation of centrosome and microtubule dynamics by proteins such as Lis1, Doublecortin, and Nudel among others (Ayala et al., 2007; Higginbotham and Gleeson, 2007; Lambert de Rouvroit and Goffinet, 2001). However, little is known about the molecular mechanisms underlying membrane dynamics during neuronal migration and morphogenesis.

The basis of neurite initiation, outgrowth, and branching is rooted in the ability of the actin and microtubule cytoskeleton to undergo dynamic changes (Gupton and Gertler, 2007; Luo, 2002; Mattila and Lappalainen, 2008). Filopodia have been shown to play a role in neurite initiation (Dent et al., 2007; Kwiatkowski et al., 2007), growth cone dynamics (Burnette et al., 2007; Gallo and Letourneau, 2004), neurite outgrowth (Luo, 2002), and branching (Dent et al., 2004; Gallo and Letourneau, 1998). Down-regulation of the actin anti-cappers ENA/VASP proteins, which are potent inducers of filopodia, resulted in failed neurite initiation and also in defects in cortical lamination (Kwiatkowski et al., 2007), suggesting a functional relationship between filopodia formation, neurite initiation, and neuronal migration.

Classically, filopodia formation is thought to be primarily dependent on proteins that regulate actin polymerization at the barbed end of actin filaments and proteins bundling F-actin (Gupton and Gertler, 2007). Interestingly, the BAR superfamily member IRSp53 has been shown to induce filopodia through membrane deformation independently of its F-actin bundling activity (Lim et al., 2008; Mattila et al., 2007; Saarikangas et al., 2009). The BAR domain superfamily contains three main groups: (1) the Bin/Amphiphysin/Rvs (BAR) domain subfamily (Itoh and De Camilli, 2006), (2) the Fes-Cip4 homology BAR (also called F-BAR or EFC) domain subfamily (Itoh et al., 2005; Tsujita et al., 2006; reviewed in Frost et al., 2009), and (3) the I-BAR subfamily (reviewed in Scita et al., 2008). Structural analysis of three F-BAR domains demonstrated that these domains are elongated homodimers characterized by a shallow curvature formed by the antiparallel interaction of two α-helical coiled coils (Henne et al., 2007; Shimada et al., 2007). In addition to sharing the general fold and quaternary organization of the BAR domain superfamily,

F-BAR domains share functional properties with "classical" BAR domains, most notably the ability to bind and deform membranes in vitro and in living cells (Frost et al., 2008; Itoh et al., 2005; Kakimoto et al., 2006; Shimada et al., 2007). However, to date, the in vivo functions of F-BAR domain-containing proteins are largely unknown (Frost et al., 2009).

Here we identify slit-robo GTPase activating protein (srGAP2) as a regulator of neuronal migration and morphogenesis through the unexpected ability of its N-terminal F-BAR domain to induce filopodia-like membrane protrusions resembling those induced by I-BAR domains. Our results highlight the functional importance of proteins directly regulating membrane deformation for proper neuronal migration and axon-dendrite morphogenesis.

RESULTS

Expression of srGAP2 in the Developing Cortex

To begin our study of the role of srGAP2 in cortical development, we first examined its pattern of expression. srGAP1–3 have recently been reported to be expressed throughout the cortex during and after radial migration (Bacon et al., 2009; Mattar et al., 2004; Yao et al., 2008). Our analysis confirmed that srGAP2 mRNA is expressed throughout the developing cortex and is found both in proliferative zones (ventricular zone [VZ] and subventricular zone [SVZ]) at embryonic day 13 (E13) and E15 and in postmitotic regions (cortical plate [CP]) at E15 and postnatal day 1 (P1) (Figure 1A). In order to determine the pattern of srGAP2 protein expression, we used a polyclonal antibody raised against the C terminus of srGAP2 (Figures 1B and 1C; Yao et al., 2008). srGAP2 protein is expressed throughout cortical development culminating at P1 corresponding to the peak of neuronal migration in the cortex. Its expression is maintained at P15 and reduced, but still present, in adult cortex (Figure 1C).

Immunofluorescent staining for srGAP2 shows that it is ubiquitously expressed in the cortical wall (Figure 1D) being found both in Nestin-positive neuronal progenitors in the VZ (Figures 1H–1J) and MAP2-positive postmitotic neurons in the CP (Figures 1E–1G). At the subcellular level, endogenous srGAP2 is found at the cell periphery (Figures 1K–1M, arrows) and was often localized along F-actin-rich filopodia-like protrusions (arrowhead in Figures 1K–1P) in acutely dissociated E15 cortical neurons.

Full-Length srGAP2 and Its F-BAR Domain Induce Filopodia Formation

Overexpression of F-BAR domain-containing proteins such as FBP17 or CIP4 have been shown to cause membrane invagination and tubulation in cell lines (Itoh et al., 2005; Tsujita et al., 2006). Surprisingly, expression of srGAP2 did not induce any membrane invaginations but instead induced filopodia formation (see Figures S1D–S1F and S1P available online). This effect requires its F-BAR domain since deletion of the F-BAR domain (srGAP2$^{\Delta F\text{-}BAR}$-EGFP) does not induce filopodia formation in COS7 cells (Figures S1G–S1I and S1P).

Interestingly, unlike the F-BAR domains of FBP17 and CIP4 (Itoh et al., 2005), expression of the F-BAR domain of srGAP2 did not inhibit endocytosis, as assessed using Alexa546-Transferrin uptake assay (Figure S2). Furthermore, expression of the isolated F-BAR domain fused to EGFP induced filopodia formation similar to full-length srGAP2 (Figures S1J, S1K, and S1P). Of note, the F-BAR domain is a potent membrane-targeting motif (Figure S1J). These data suggest that the F-BAR domain of srGAP2 is necessary and sufficient for membrane localization and the induction of filopodia-like membrane protrusions.

In order to distinguish the membrane-targeting function of the F-BAR domain from its membrane deformation activity, we identified a small truncation of the last C-terminal 49 amino acids (F-BAR$^{\Delta 49}$) (Figure S3A and Supplemental Experimental Procedures for details). Expression of F-BAR$^{\Delta 49}$-EGFP results in significant membrane targeting (Figure S4) but fails to induce filopodia in COS7 cells (Figures S1M–S1P). We do not currently know the structural basis for the inability of this truncation to elicit filopodia but we can at least exclude two possibilities: (1) instability of the F-BAR$^{\Delta 49}$ protein since it expresses at a level comparable to full-length srGAP2 or its F-BAR domain in cells (Figure S5) and (2) this truncation does not disrupt its dimerization properties since F-BAR$^{\Delta 49}$ can dimerize with F-BAR or full-length srGAP2 (data not shown). Interestingly, these 49 amino acids reside in an extension specific to the srGAP subfamily (α6–8; Figure S3A) that is C-terminal to the minimal, predicted F-BAR domain (amino acids 1–358; Itoh et al., 2005) (Figure S3B). Indeed, we were unable to obtain stable protein expression of this minimal predicted F-BAR domain (amino acids 1–358) in mammalian cells or bacteria (data not shown). Furthermore, as shown for other F-BAR domains (Frost et al., 2008; Itoh et al., 2005; Kakimoto et al., 2006; Shimada et al., 2007), srGAP2 forms a stable dimer in solution as assessed by light scattering assays (Figure S3C), and deletion of the Fes-Cip4 homology (FCH) domain (green box in Figure S3A), which represents a significant portion of the dimerization interface, abolishes the ability of srGAP2 to induce filopodia in COS7 cells (data not shown). Altogether, these data suggest that all eight predicted α helices are likely to be required for formation of the functional F-BAR domain of srGAP2.

The F-BAR Domain of srGAP2 Deforms Membrane Like an I-BAR Domain

The ability of srGAP2 or its F-BAR domain to induce filopodia in COS7 cells is reminiscent of the activity of the structurally related I-BAR domain-containing proteins (Mattila et al., 2007; Millard et al., 2007; Saarikangas et al., 2009; Scita et al., 2008). Interestingly, F-actin depolymerization prevents the dynamics and formation of new filopodia but does not affect the maintenance of preexisting filopodia induced by the I-BAR domains of IRSp53 or MIM (Mattila et al., 2007). We found the same results for the F-BAR domain of srGAP2 (Figures 2A–2C), while cells treated with cytochalasin D were depleted of F-actin. Strikingly, this treatment had no effect on membrane localization of the F-BAR domain or on the maintenance of filopodia-like protrusions (Figures 2D–2F). F-BAR-induced filopodia were highly dynamic in COS7 cells (Figures 2G–2J and Movie S1). Treatment with cytochalasin D significantly impaired the extension and retraction of F-BAR-induced filopodia (Figures 2K–2N and Movie S2), suggesting that F-actin is required for the dynamics of these protrusions.

In order to directly test the membrane deformation properties of the F-BAR domain of srGAP2, we incubated purified F-BAR

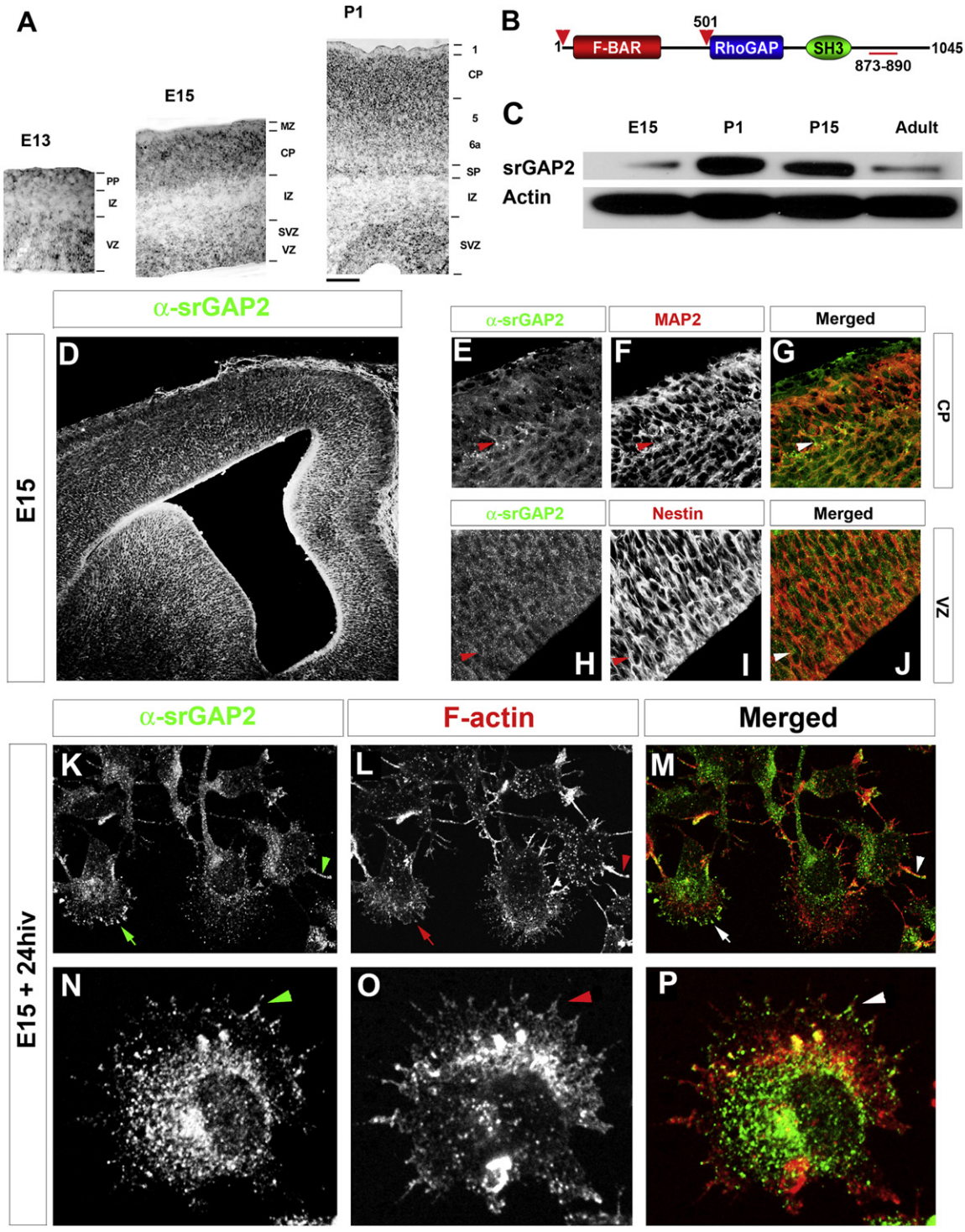

Figure 1. srGAP2 Is Expressed in Neuronal Progenitors and Postmitotic Neurons and Localizes to Sites of Membrane Protrusion

(A) In situ hybridization for srGAP2 in developing cortex at E13, E15, and P1.

(B) Domain organization of srGAP2, which contains an F-BAR domain, a RhoGAP, and a SH3 domain from N- to C-terminal ends (1–1045 amino acids, predicted molecular weight of 118 kDa). The red bar indicates the localization of the antigen (A2; amino acids 873–890) used to affinity purify the srGAP2-specific polyclonal antibody to the C terminus of srGAP2.

(C) Western blot for srGAP2 protein levels during cortical development at the indicated time points (E15, P1, P15, and Adult) obtained by SDS-PAGE and immunoblotting with A2-rabbit polyclonal antibody.

domain with preformed liposomes. As visualized by negative stain transmission electron microscopy, this did not result in liposome outward tubulation as has been reported for other F-BAR domains (see Figure S5B). Rather, the F-BAR domain of srGAP2 induced an inward dimpling or "scalloping" of the liposome surface (Figures 2O and 2P), which is reminiscent of the activity of I-BAR domains in the same conditions (Suetsugu et al., 2006), suggesting that the F-BAR domain of srGAP2 can induce "inverse" membrane tubulation.

These results suggested the possibility that if the purified F-BAR domain of srGAP2 could be exposed to the inside surface of liposomes, then protrusive tubules would form (Figure 2Q). To test this hypothesis, mixtures of the F-BAR domain with intact, large unilamellar vesicles (LUVs) were briefly sonicated, which presumably resulted in transient pore formation in liposomes and introduction of the recombinant F-BAR inside LUVs. Following a wash, liposomes were fixed, negatively stained, and imaged using transmission electron microscopy. As predicted by the I-BAR model, this resulted in numerous long tubular extensions emerging from LUVs (Figure 2R), which is in stark contrast with control sonicated liposomes not incubated with recombinant protein (Figure S6A). Consistent with the dimensions of tubules induced by other members of the F-BAR and I-BAR families (Frost et al., 2008; Mattila et al., 2007), the srGAP2 F-BAR-induced tubules were 83 nm ± 15 nm (average ± SD, n = 38) in diameter. Importantly, at higher magnification, the tubules observed by negative staining electron microscopy after sonication do not have an obvious protein coat surrounding the liposomes (Figure 2R). This is in contrast with tubules induced by other F-BAR and BAR domains that coat the outer surface of the tubule (Figure S6B; Frost et al., 2008; Shimada et al., 2007). Together, these results suggest that unlike previously characterized F-BAR domains, the F-BAR domain of srGAP2 functions as an I-BAR domain (Mattila et al., 2007; Suetsugu et al., 2006).

srGAP2 Regulates Neurite Formation and Branching through the Ability of Its F-BAR Domain to Form Filopodia

We next tested the function of srGAP2 in neuronal morphogenesis by designing short hairpin interfering RNA (shRNA) in order to acutely knock down srGAP2 expression (Figure 3A). We found that srGAP2 knockdown in E15 cortical neurons led to a significant decrease in both axonal (Figures 3C, 3D, and 3F) and dendritic branching after 5 days in vitro (DIV) (Figures 3G, 3H, and 3J). Both of these effects were rescued by cotransfection of a shRNA-resistant form of srGAP2 (srGAP2*; Figures 3B, 3E, 3F, 3I, and 3J), demonstrating that this is not an off-target effect. The fact that srGAP2 knockdown reduced branching in cortical neurons, a process previously shown to require filopodia formation (Dent et al., 2004; Gallo and Letourneau, 1998), suggests that srGAP2 may promote neurite branching through its ability to induce filopodia in neurons.

To test this hypothesis, we performed a structure/function analysis using electroporation of E15 cortical progenitors with various srGAP2 constructs followed by dissociation and culture, which induces rapid differentiation. First, we restricted our analysis to stage 1 neurons (Dotti et al., 1988), when immature postmitotic neurons produce a significant number of filopodia-like protrusions (Dent et al., 2007; Kwiatkowski et al., 2007). Our analysis shows that expression of full-length srGAP2 induced a significant increase in filopodia-like protrusions in stage 1 cortical neurons compared to control EGFP (Figures 4A–4C and 4F). This effect requires the F-BAR domain since deletion of the F-BAR domain (srGAP2$^{\Delta F\text{-}BAR}$) significantly reduced the ability of srGAP2 to induce filopodia in stage 1 neurons (Figures 4C and 4F). As in COS7 cells, expression of the F-BAR domain alone potently induces formation of F-actin-rich filopodia (Figures 4D and 4F). Again, the effect of the F-BAR domain requires its membrane deformation properties and not simply its membrane targeting property since expression of F-BAR$^{\Delta 49}$ does not induce filopodia in stage 1 cortical neurons (Figures 4E and 4F) and instead induces large lamellipodia (arrowhead in Figure 4E). These data suggest that srGAP2, through its F-BAR domain, induces filopodia in cortical neurons as shown in COS7 cells.

We then analyzed stage 2 neurons, i.e., prior the emergence of a single axon (Dotti et al., 1988), in order to test if srGAP2 and its F-BAR domain were sufficient to promote the transition between filopodia and elongating neurites defined by the presence of bundled microtubules (see also Figure S7 for isolated βIII-tubulin signal). Both full-length srGAP2 and the F-BAR domain significantly increased the total number of primary neurites emerging from the cell body (Figures 4G–4K) as well as the number of primary neurite branches (Figure 4L). Expression of srGAP2$^{\Delta F\text{-}BAR}$ as well as F-BAR$^{\Delta 49}$ fails to increase primary neurite number and neurite branching compared to control (Figures 4J–4L).

Reduction of srGAP2 Expression Promotes Neuronal Migration

To determine the function of srGAP2 during cortical development, we introduced our shRNA constructs directed against srGAP2 (Dha2 and Dha5; Figure 3A) into radial glial progenitors at E15 using ex vivo cortical electroporation coupled with organotypic slice culture (Hand et al., 2005). Interestingly, after 3 days in culture, at a time point when few control shRNA electroporated neurons have already migrated (Figures 5A, 5C, and 5D), slices expressing srGAP2 shRNA showed a significant increase in the percentage of neurons that have reached the dense CP and a corresponding decreased percentage of neurons in the intermediate zone (IZ) (Figures 5B–5D), suggesting that reduction of srGAP2 expression accelerated radial migration. To test this directly, we used time-lapse confocal microscopy to visualize neurons coexpressing nuclear EGFP (to ease cell tracking) and control shRNA (Figures 5E–5H and Movie S3) or srGAP2 shRNA (Figures 5E–5L and Movie S4) in slice culture. We found

(D–J) Immunofluorescence staining of srGAP2 protein expression on fixed coronal sections of E15 mouse cortex. srGAP2 protein colocalizes (arrowheads) with MAP2 (postmitotic neuron marker) in the CP (D–F) and also colocalizes with Nestin (arrowheads) (neuronal precursor marker) in the VZ (G–I).
(K–P) Immunofluorescence staining of srGAP2 protein in early dissociated cortical neuron cultures (E15+ 24 hr in vitro [hiv]). srGAP2 protein is found close to the plasma membrane of immature cortical neurons (arrow in K–M) and to F-actin-rich filopodia (stained with Alexa546-phalloidin; arrowheads in K–P).

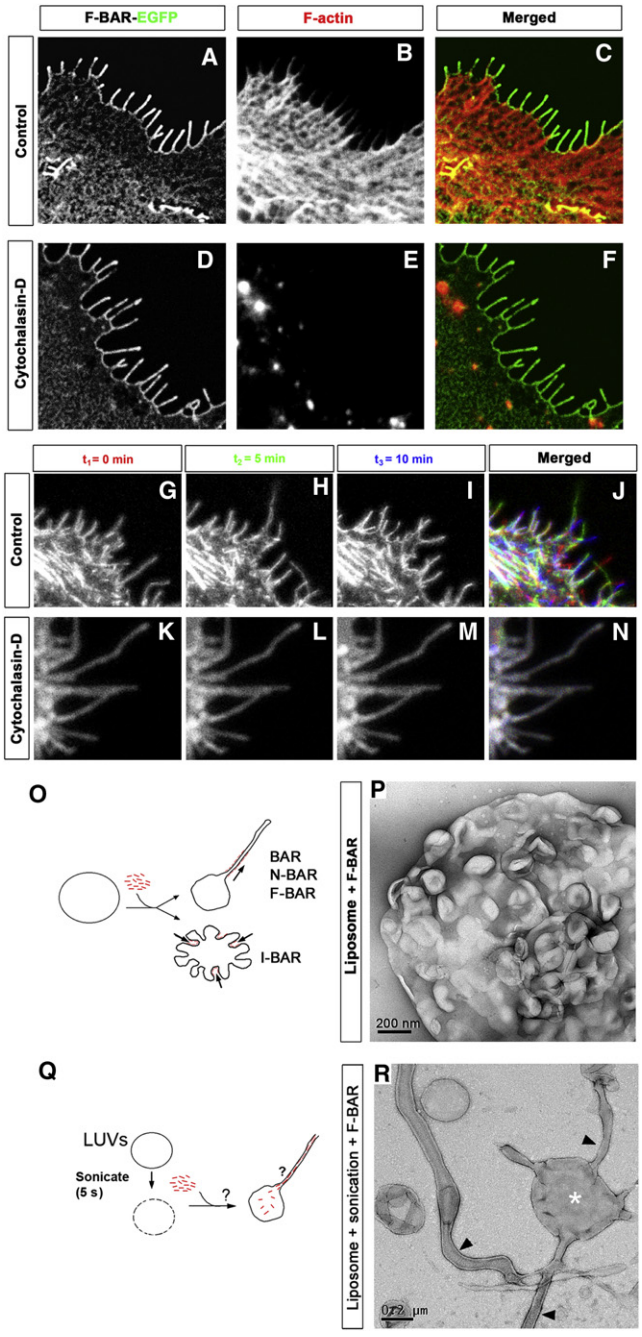

Figure 2. F-BAR-Induced Filopodia Required F-Actin for Their Dynamic Formation but not for Their Structural Maintenance

(A–C) COS7 cell expressing the F-BAR-EGFP fusion protein not treated with cytochalasin D (control). Note the cortical localization of the F-BAR domain and the numerous F-actin-rich filopodia (phalloidin in B and C).

(D–F) COS7 cell expressing the F-BAR-EGFP fusion protein incubated with 400 μM cytochalasin D for 30 min. Note that the complete loss of F-actin (phalloidin) (E) had no effect on the localization of the F-BAR domain or on the structure of the F-BAR-mediated protrusions.

(G–J) Time series showing the dynamics of F-BAR-EGFP-induced filopodia in COS7 cells. Time 0, 5, and 10 min are pseudocolored in red, green, and blue, respectively. Note that there is little colocalization of filopodia at the cell periphery (J). This is in stark contrast to COS7 cells expressing F-BAR-EGFP treated with cytochalasin D (30 min) (K–N), where the protrusions remain static and do not grow or retract for the same period of time shown in control cells.

(O) Schema depicting tubulation assay in (P).

(P) F-BAR domain of srGAP2 added to preformed liposomes. Note the inward dimpling or "scalloping" of the liposome surface.

(Q) Schema depicting tubulation assay in (R) where F-BAR domain of srGAP2 was added to liposomes after extrusion. This results in a fraction of the F-BAR domain resident inside the liposome. Note the formation of tubule protrusion from the liposome.

(R) High magnification of liposome/F-BAR mixture after sonication. Note the absence of striations or an obvious protein coat on the lipid tubule, a hallmark of canonical F-BAR tubulation. These tubules are 83 nm ± 15 nm (average ± SD, n = 38) after being partially flattened by the negative staining procedure.

that srGAP2 shRNA-expressing neurons migrated 25% faster than those expressing control shRNA (Figure 5M), suggesting that reduction of srGAP2 increased the actual rate of cell translocation.

Excessive LP branching in migrating cortical neurons can inhibit neuronal migration (Gupta et al., 2003; Ohshima et al., 2007). Indeed, the LP of srGAP2 knockdown neurons in layers 5/6 was significantly less branched compared to control shRNA neurons (Figures 5N–5P). These data suggest that srGAP2 may negatively regulate the rate of radial migration by promoting LP branching and dynamics.

The F-BAR Domain Is Necessary and Sufficient for srGAP2-Mediated Inhibition of Radial Migration

We hypothesized that overexpression of srGAP2 or its F-BAR domain should be sufficient to block migration by increasing filopodia formation and LP dynamics. Indeed, overexpression of srGAP2 severely inhibited radial migration compared to control EGFP-expressing slices electroporated at E15 and cultured for 5 DIV (Figures 6E–6H). We quantified radial migration by determining the ratio of neurons in the dense CP (where pyramidal neurons complete migration) and in the IZ, where they initiate radial migration (see Figure S8 for definition of cytoarchitecture). This CP/IZ ratio (Figure 6U) is significantly decreased by srGAP2 overexpression (Figures 6E–6H) when compared to control EGFP-expressing neurons (Figures 6A–6D), demonstrating that srGAP2 overexpression inhibits neuronal migration. Expression of srGAP2$^{\Delta F\text{-}BAR}$ did not significantly reduce the CP/IZ ratio compared to EGFP control (Figures 6I–6L and 6U) and is significantly different from the ratio measured by srGAP2 overexpression (Figure 6U), suggesting that the F-BAR domain is partially required for srGAP2's ability to inhibit migration. Moreover, expression of the F-BAR domain alone was sufficient to reduce neuronal migration to the same extent as srGAP2 while expression of F-BAR$^{\Delta 49}$ had no effect on the ability of neurons to migrate (Figures 6M–6U), suggesting that the ability of the F-BAR domain to induce filopodia is required for the ability of srGAP2 to inhibit neuronal migration.

srGAP2 Inhibits Migration by Increasing Leading Process Dynamics and Branching

The accumulation of neurons expressing srGAP2 or its F-BAR domain in the IZ suggested that the neurons might be partially blocked in the multipolar to unipolar transition (Noctor et al., 2004). Indeed quantification of the percentage of multipolar cells

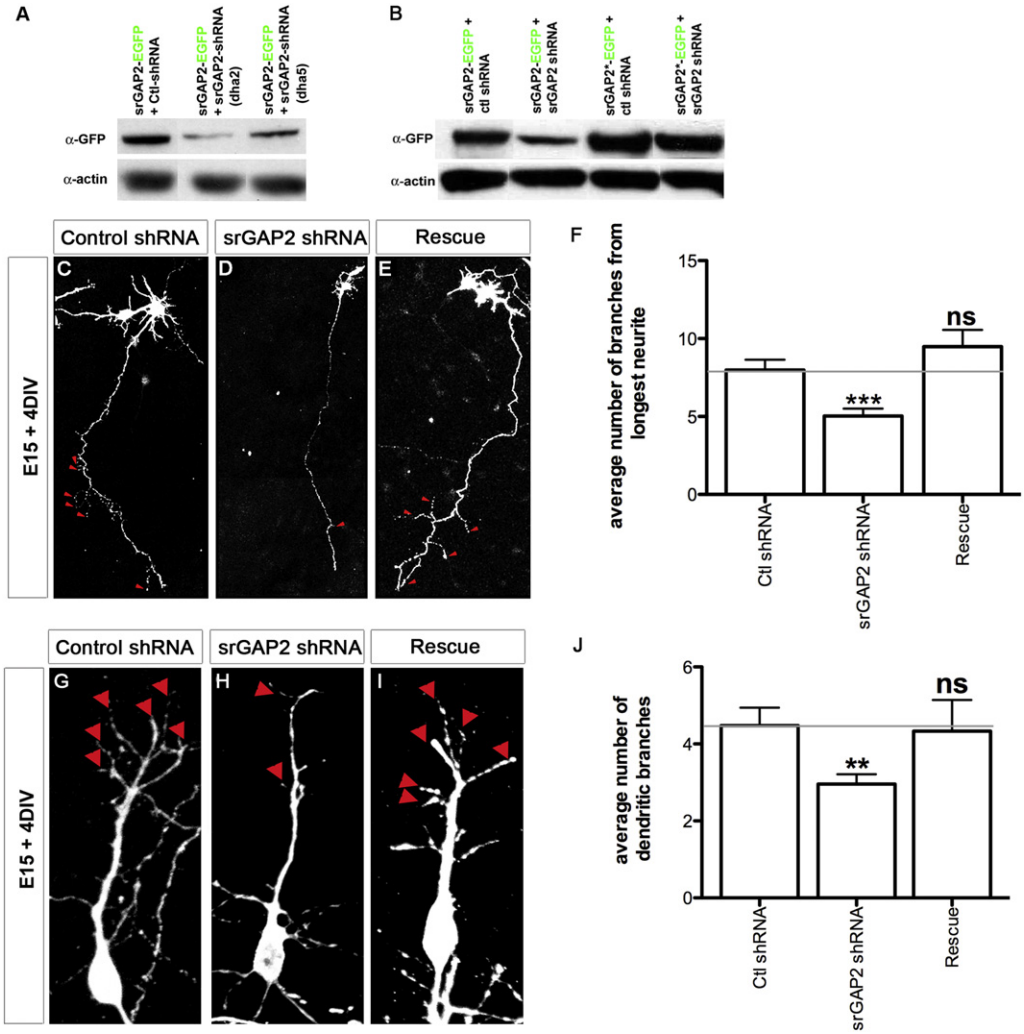

Figure 3. Knockdown of srGAP2 in Cortical Neurons Reduces Axonal and Dendritic Branching

(A) Western blot probed with anti-GFP and anti-actin antibodies from COS7 cells cotransfected with either control shRNA plus srGAP2-EGFP (lane 1), srGAP2 shRNA plus srGAP2-EGFP (Dha2, lane 2), or srGAP2 shRNA plus srGAP2-EGFP (Dha5, lane3).

(B) Western blot probed with anti-GFP and anti-actin antibodies from COS7 cells cotransfected with either control shRNA plus srGAP2-EGFP (lane 1), srGAP2 shRNA plus srGAP2-EGFP (lane 2), a mutated form of srGAP2*-EGFP (resistant to srGAP2 shRNA) plus control shRNA (lane 3), or srGAP2*-EGFP plus srGAP2 shRNA (lane 4). srGAP2 shRNA significantly knocks down srGAP2 expression compared to control shRNA, which can be rescued by expression of srGAP2*-EGFP (compare lanes 3 and 4).

(C–E and G–I) E15 dissociated cortical neurons were cultured for 5 days after ex vivo cortical electroporation (EVCE) with control shRNA, srGAP2 shRNA, or srGAP2 shRNA + srGAP2*-EGFP. Control shRNA-transfected neurons display frequent primary branches from the axon (arrowheads in B) and the primary dendrite (arrowheads in F). Both effects were markedly reduced in srGAP2 shRNA-transfected neurons (D and H) and rescued by cotransfection of srGAP2 shRNA with srGAP2*-EGFP (E and I).

(F) Quantification of the number of branches from the longest neurite (axon) as shown in (C)–(E).

(J) Quantification of the number of primary dendritic branches as shown in (G)–(I). Control shRNA, n = 42 cells; srGAP2 shRNA, n = 95; srGAP2*-EGFP + srGAP2 shRNA, n = 39. Cells were taken from three independent experiments and analyzed blind to the treatment.

Mann-Whitney Test: *$p < 0.05$; **$p < 0.01$; ***$p < 0.001$.

(cells displaying three or more neurites) in the IZ of slices electroporated with srGAP2 or the F-BAR domain revealed a significant increase in the percentage of neurons with multiple processes emerging from the cell body compared to control (Figure 6V). This is consistent with the ability of srGAP2 to induce filopodia and neurite initiation/branching in dissociated neurons (see Figure 4).

Our time-lapse confocal microscopy analysis shows that control neurons in the IZ form a stable LP upon initiating radial migration (green arrowheads in Figure 6W and Movie S5) and undergo efficient cell body translocation (green arrows in Figure 6W and Movie S5). In contrast, neurons overexpressing srGAP2 or the F-BAR domain alone do not undergo cell body translocation (red arrows in Figures 6X and 6Y and Movies S6

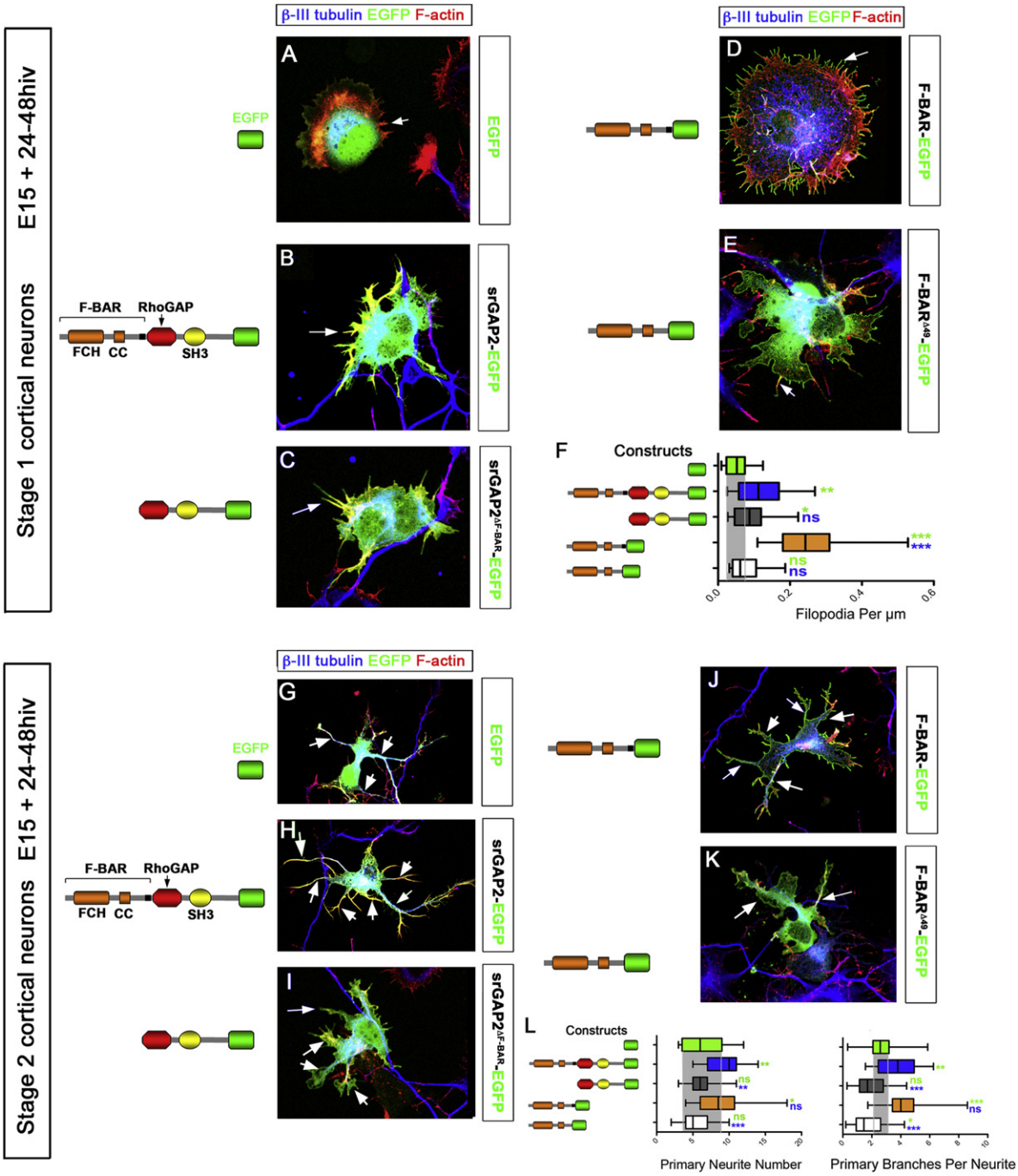

Figure 4. srGAP2 Promotes Filopodia Formation and Neurite Outgrowth in an F-BAR-Dependent Manner

(A–E) Stage 1 cortical neurons expressing various srGAP2 constructs. All cells are stained with neuron-specific βIII-tubulin (blue) to reveal presence of microtubules (see also Figure S7) and phalloidin (red) to visualize F-actin.

(F) Quantification of filopodia normalized per cell perimeter in all conditions. EGFP, n = 20 cells; srGAP2-EGFP, n = 21; srGAP2$^{\Delta F\text{-}BAR}$-EGFP, n = 20; F-BAR-EGFP, n = 20; F-BAR$^{\Delta 49}$-EGFP, n = 20. Cells were taken from three independent experiments and analyzed blind to the treatment.

(G–K) Stage 2 cortical neurons expressing various srGAP2 constructs. All cells are stained with βIII-tubulin (blue) and phalloidin (red) as in panels (A)–(F). Arrows point to primary neurites.

(L) Quantification of neurite number normalized per cell perimeter in all conditions and primary branch number per neurite. Note srGAP2 and F-BAR are potent inducers of neurite outgrowth while srGAP2 $^{\Delta\ F\text{-}BAR}$ and F-BAR $^{\Delta 49}$ are not. Mann-Whitney test: *p < 0.05; **p < 0.01; ***p < 0.001. Green stars indicates comparison to EGFP and blue stars indicates comparison to srGAP2-EGFP.

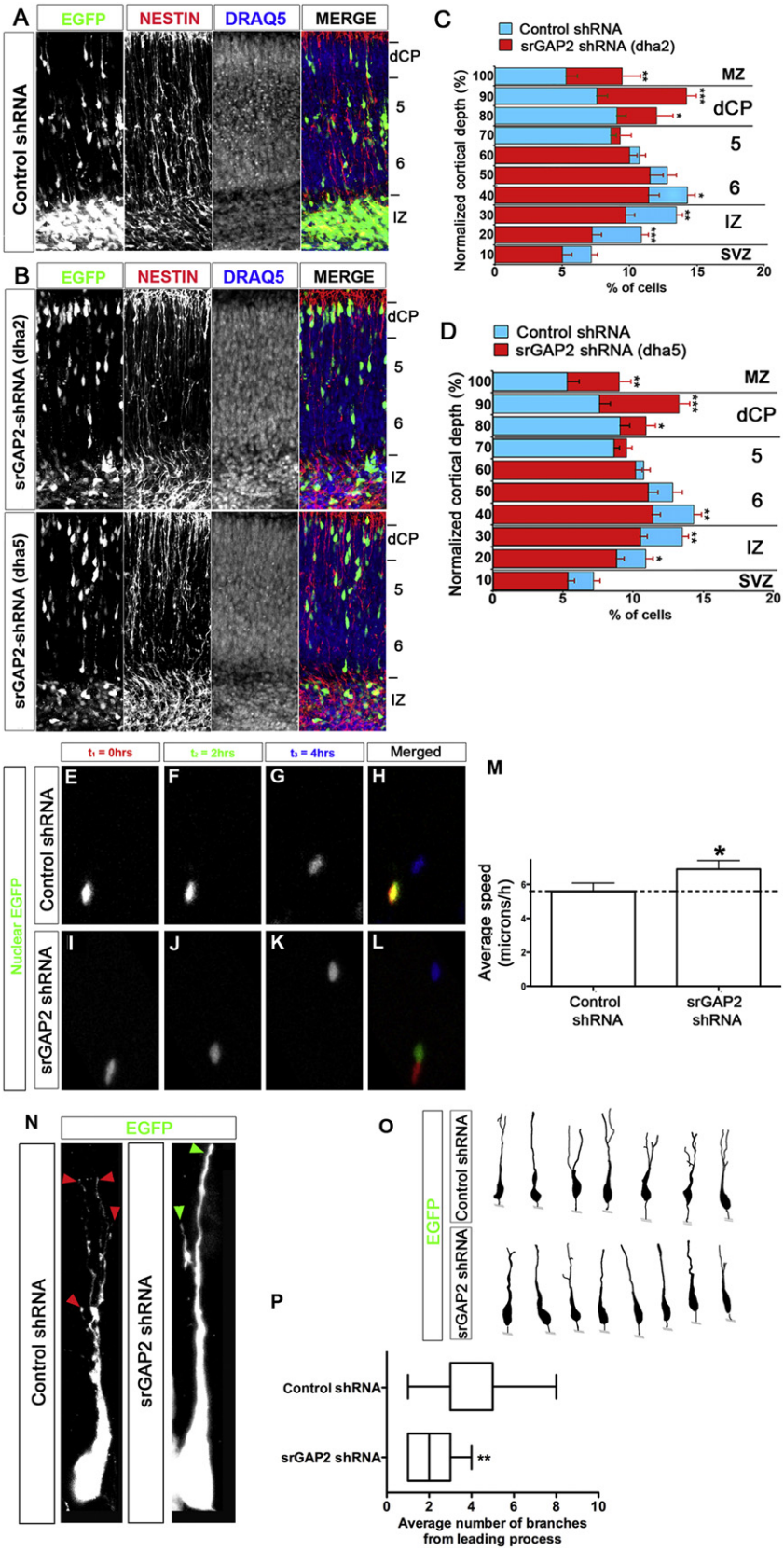

Figure 5. Knockdown of srGAP2 Promotes Neuronal Migration and Reduces LP Branching

(A) E15 cortical slices cultured for 3 days after electroporation with EGFP + control shRNA. Slices were stained with anti-Nestin antibody revealing radial glial scaffold and Draq5 to illustrate cytoarchitecture.

(B) E15 cortical slices cultured for 3 days after electroporation with EGFP + Dha2 (B, top panel) or Dha5 (B, lower panel). Slices were stained with anti-Nestin antibody, revealing radial glial scaffold and Draq5 to illustrate cytoarchitecture.

(C and D) Quantification of cell distribution for slices expressing control shRNA (blue bars) and two independent srGAP2 shRNA (red in C and D for dha2 and dha5, respectively).

(E–L) E15 cortical slices cultured for 2 days ex vivo after electroporation with nuclear EGFP (3NLS) along with control shRNA (E–H) or srGAP2 shRNA (I–L) were imaged using time-lapse confocal microscopy. Neurons transfected with srGAP2 shRNA undergo faster translocation within 4 hr (I–L; and no colocalization in L) than control shRNA-transfected neurons.

(M) Quantification of effects of srGAP2 knockdown on cell speed. Neurons with reduced level of srGAP2 (shRNA) migrated approximately 25% faster (6.91 μm/hr compared to 5.59 μm/hr) compared to control shRNA-transfected neurons. Control shRNA, n = 95 cells; srGAP2 shRNA, n = 84. Cells were taken from three independent experiments. Mann-Whitney test: *p < 0.05; **p < 0.01; ***p < 0.001.

(N–O) High magnification images (N) and reconstructions (O) of control shRNA (left panel) or srGAP2 shRNA (right panel) expressing neurons in layers 5/6. Arrowheads point to LP tips.

(P) Quantification of the LP branch number in control shRNA or srGAP2 shRNA expressing neurons. Control shRNA, n = 19 cells; srGAP2 shRNA, n = 17 cells. Cells were taken from three independent experiments. Mann-Whitney test: *p < 0.05; **p < 0.01; ***p < 0.001.

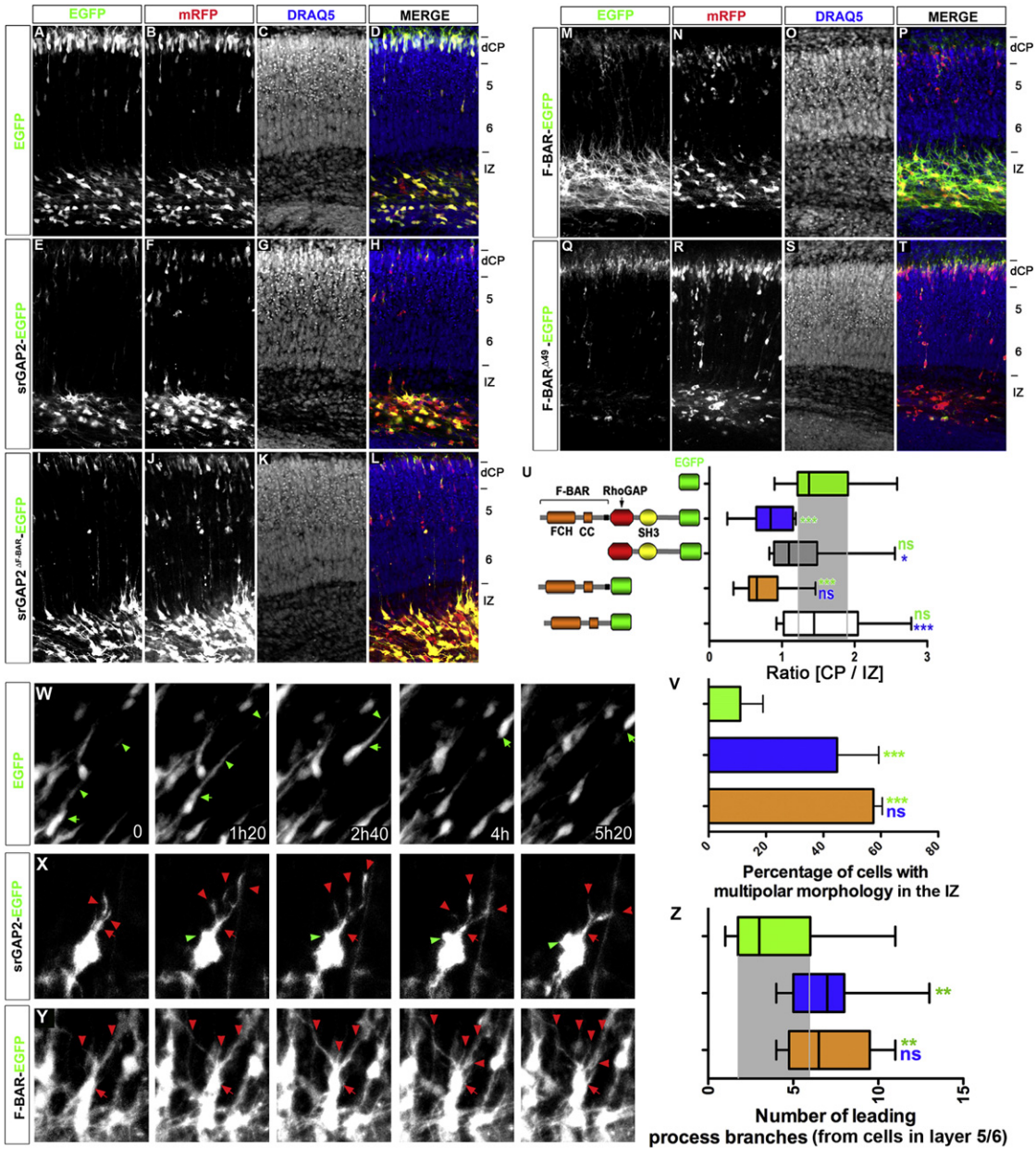

Figure 6. srGAP2-Mediated Inhibition of Migration Requires F-BAR-Mediated Membrane Deformation

(A–T) E15 cortical slices cultured for 5 days after coelectroporation of monomeric red fluorescence protein (mRFP for cytoplasmic filing) together with EGFP (A–D), full-length srGAP2-EGFP (E–H), srGAP2$^{\Delta F\text{-}BAR}$-EGFP (I–L), F-BAR-EGFP (M–P), and F-BAR$^{\Delta 49}$-EGFP fusion proteins (Q–T).

(U) Quantification of CP/IZ ratio. EGFP, n = 13 slices; srGAP2-EGFP, n = 14 slices; srGAP2$^{\Delta F\text{-}BAR}$-EGFP, n = 8 slices; F-BAR-EGFP, n = 10 slices; F-BAR$^{\Delta 49}$-EGFP, n = 6 slice. Slices were taken from four different experiments and CP/IZ ratio was analyzed using Mann-Whitney test: *p < 0.05; **p < 0.01; ***p < 0.001. Green stars indicate comparison to EGFP and blue stars indicate comparison to srGAP2-EGFP.

(V) Quantification of percentage of cells with multipolar morphology in EGFP, srGAP2-EGFP, or F-BAR-EGFP transfected slices. Multipolar cells were defined as cells possessing three or more processes. EGFP, n = 66 cells; srGAP2-EGFP, n = 42; F-BAR-EGFP, n = 57. Cells were taken from three different experiments and analyzed using Fisher's exact test: *p < 0.05; **p < 0.01; ***p < 0.001.

(W–Y) Individual frames using time-lapse confocal microscopy of E15 cortical slices cultured for 3 days after electroporation with EGFP, srGAP2-EGFP, or F-BAR-EGFP (cotransfected with Venus plasmid). Arrows indicate LP and arrowheads indicate the cell body.

(Z) Quantification of LP branch number from cells expressing EGFP, srGAP2-EGFP, or F-BAR-EGFP in layer 5/6. EGFP, n = 17 cells; srGAP2-EGFP, n = 21 cells; F-BAR-EGFP, n = 9 cells. Cells were taken from three independent slices. Mann-Whitney test: *p < 0.05; **p < 0.01; ***p < 0.001. Green stars indicate comparison to EGFP and blue stars indicate comparison to srGAP2-EGFP.

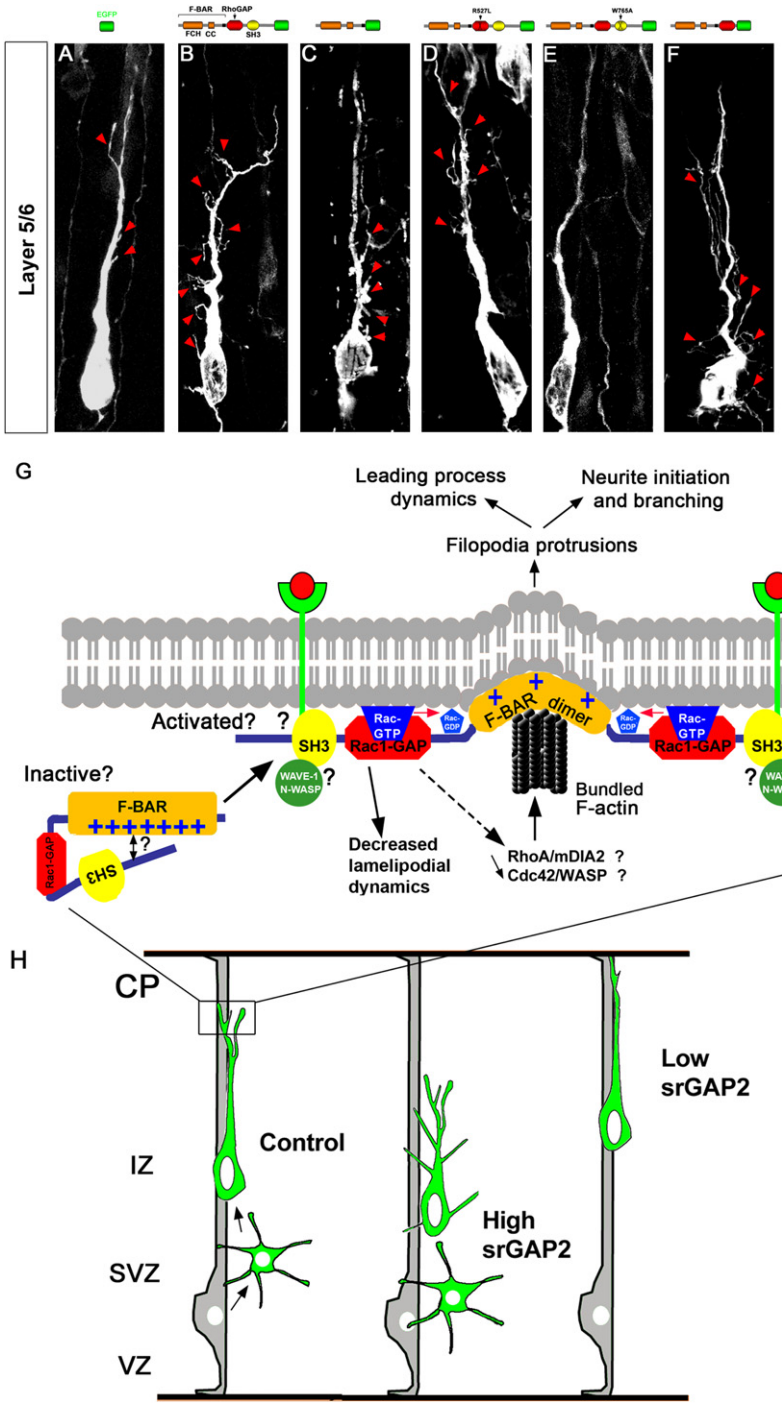

Figure 7. Model for srGAP2-Regulated Membrane Protrusion in Neuronal Migration

(A–F) Representative images of optically isolated neurons translocating radially through layer 5/6 following electroporation at E15 (+5 DIV) with indicated srGAP2 constructs containing an F-BAR domain.

(G and H) Hypothetical model of the molecular mechanisms underlying srGAP2 function in membrane protrusion during neuronal migration and morphogenesis (G). Summary of srGAP2 effects on neuronal migration and morphogenesis during cortical development (H). See text for details.

and S7) and instead form multiple processes that are highly dynamic and unstable (red arrowheads in Figures 6X and 6Y and Movies S6 and S7). The plasma membrane of these cells appears highly dynamic showing large, transient protrusions (green arrowheads in Figure 6X). While many neurons accumulate in the IZ, some did manage to translocate into layers 5/6 (Figures 6E–6H and 6M–6P), where expression of srGAP2 or its F-BAR domain significantly increases LP branching compared to EGFP control (Figure 6Z and Figures 7A–7C). Together, these data suggest that srGAP2 increases neurite initiation and branching through the ability of its F-BAR domain to induce filopodia, which in turn negatively regulates neuronal migration.

Finally, to ensure that the ability of srGAP2 expression to inhibit migration was not due to an indirect effect of srGAP2 expression on progenitor cell cycle exit, we designed a vector allowing us to express srGAP2 in early postmitotic neurons using the 2.2 kB NeuroD promoter (Figure S9A). NeuroD is a bHLH transcription factor and a direct transcriptional target of Ngn2 (Hand et al., 2005; Heng et al., 2008), thereby inducing cDNA expression in intermediate progenitors and early postmitotic neurons in the subventricular zones and IZ (Figures S10E–S10H) but not by Nestin+ radial glial progenitors in the VZ as obtained by the chicken β-actin promoter (Figures S10A–S10D). Furthermore, the level of protein expression in neurons obtained with this promoter is significantly lower than using the chicken β-actin promoter (data not shown; Heng et al., 2008). Expression of srGAP2 using this NeuroD promoter significantly reduced the number of cells reaching the CP compared to control (Figures S9B–S9J).

srGAP2 Partially Requires Its RhoGAP and SH3 Domains to Inhibit Migration

We next wanted to determine the contributions of the RhoGAP and SH3 domains to srGAP2 function in neuronal migration and morphogenesis. In order to determine the substrate specificity of the GAP domain of srGAP2, we purified its GAP domain as a GST fusion (Figure S11A). We then performed fluorescence-based GTP hydrolysis assays (Figure S11B; Shutes and Der, 2006). The GAP domain of srGAP2 increased the rate of GTP hydrolysis on Rac1, but had no effect on RhoA or Cdc42 (Figure S11B) or RhoG (data not shown). In addition, full-length srGAP2 strongly interacted with activated Rac1 ($Rac1^{Q61L}$) but

only weakly interacted with activated Cdc42^{Q61L} (Figure S11C) and activated RhoA^{Q63L} (data not shown). These two independent approaches demonstrate that the GAP domain of srGAP2 is specific for Rac1.

To determine the contribution of the Rac1-GAP domain on srGAP2's ability to regulate neuronal morphogenesis and migration, we engineered a catalytically inactive form of srGAP2 (srGAP2^{R527L}). Indeed this mutant was unable to accelerate GTP hydrolysis of Rac1 (Figure S11D). Expression of the "GAP-dead" srGAP2^{R527L} was as potent as srGAP2 at inducing filopodia-like membrane protrusions in stage 1 cortical neurons (compare Figures S12B and S12C; quantified in Figure S12F) and at promoting primary neurite initiation (Figures S12H and S12I; quantified in Figure S12L). While this mutation was competent to increase neurite initiation, there were significantly fewer (2-fold) srGAP2^{R527L}-expressing neurons at stage 2 when compared to srGAP2 (Figure S13). In addition, srGAP2^{R527L} displays a reduced ability to induce neurite branching when compared to srGAP2 (Figure S12L), suggesting that the Rac1-GAP activity of srGAP2 might participate in its function in neurite branching.

We tested the contribution of the Rac1-GAP activity of srGAP2 in its ability to inhibit neuronal migration by expressing srGAP2^{R527L} in E15 cortical progenitors. This significantly inhibited migration compared to control EGFP (Figures S14A–S14D, S14I–S14L, and S14U) although not as potently as full-length srGAP2 (Figures S14E–S14H and S14U), suggesting that the Rac1-GAP activity of srGAP2 contributes to its ability to inhibit migration. In addition, similarly to srGAP2, expression of srGAP2^{R527L} increased the percentage of multipolar cells in the IZ (Figure S14V) and increased LP branching of radially migrating neurons in layer 5/6 (Figures S14X and 6Z). These data suggest that the Rac1-GAP activity may act to modulate protrusion formation induced by the F-BAR domain of srGAP2, but is not absolutely required to induce filopodia-like membrane protrusions and inhibit neuronal migration.

To test the contribution of the SH3 domain of srGAP2, we engineered a mutant to a conserved tryptophan residue (srGAP2^{W765A}), which was shown to be required for the ability of the SH3 domain of srGAP1 to bind to Robo1 and for the SH3 domain of srGAP3 to bind to WAVE-1 (Wong et al., 2001; Li et al., 2006; Soderling et al., 2002). Expression of srGAP2^{W765A}, unlike the expression of full-length srGAP2 or its F-BAR domain, did not efficiently induce filopodia-like membrane protrusions in stage 1 cortical neurons (Figures S12D and S12F) and had a significantly decreased ability to induce primary neurite branching compared to full-length srGAP2 (Figures S12J and S12L). Expression of srGAP2^{W765A} increased primary neurite initiation, but showed a significantly reduced percentage (2-fold) of neurons transitioning from stage 1 to stage 2 compared to srGAP2 (Figure S13), suggesting that all functional domains of srGAP2 are required for its ability to promote the transition from a filopodia to an elongating neurite.

Interestingly, expression of srGAP2^{W765A} had no effect on cortical neuron migration (Figures S14M–S14P and S14U), although there was a slight increase in cells with multipolar morphology in the IZ compared to EGFP (Figure S14V). The lack of effect of srGAP2^{W765A} overexpression on the CP/IZ ratio prompted us to use time-lapse microscopy to observe LP dynamics in radially migrating neurons. This analysis revealed that migrating neurons expressing srGAP2^{W765A} did not display increased LP branching but instead had a single, stable LP (red arrowheads in Figure S14W and Movie S8) and translocated efficiently (green arrowheads in Figure S14W and Movie S8), which is strikingly different from neurons overexpressing full-length srGAP2 (Figure 6X). Moreover, analysis of neurons in layer 5/6 showed no significant increase in LP branching as demonstrated with other constructs containing an F-BAR domain (Figures 6, 7E, and S14X).

The fact that srGAP2^{W765A} showed weak filopodia formation compared to full-length srGAP2 and no increase in neurite branching suggested that the F-BAR domain might be inhibited in srGAP2^{W765A}. By analogy to the mode of activation of other RhoGAP and RhoGEF proteins (Eberth et al., 2009; Mitin et al., 2007; Yohe et al., 2007), we hypothesized that srGAP2 might normally be in an autoinhibited conformation through structural interaction between the N-terminal F-BAR domain and the C-terminal region (including the SH3 domain) that is released upon effector binding to its SH3 domain (see model in Figure 7G).

To test this model, we generated a C-terminal deletion of srGAP2 (srGAP2$^{\Delta C\text{-term}}$), which deletes the entire C-terminal portion starting from the SH3 domain to the C-terminal end. Expression of srGAP2$^{\Delta C\text{-term}}$ potently induced filopodia formation in stage 1 neurons (Figures S12E and S12F) and neurite outgrowth and branching in stage 2 neurons (Figures S12K and S12L). In sharp contrast to srGAP2^{W765A}, expression of srGAP2$^{\Delta C\text{-term}}$ potently inhibited migration (Figures S14Q–S14U) resulting in increased multipolar cells in the IZ (Figure S14V) as well as increased LP branching of migrating neurons in layer 5/6 similarly to other F-BAR-containing constructs but unlike srGAP2^{W765A} (Figures S14X and 7F).

DISCUSSION

srGAP2 Is a Novel F-BAR Domain-Containing Protein

It is well established that cytoskeletal dynamics produce forces to generate plasma membrane protrusions and invaginations; however, recent evidence suggests that many membrane-associated proteins directly sculpt and deform biological membranes (Doherty and McMahon, 2008). Here we report that srGAP2 regulates neuronal migration as well as neurite initiation and branching through the ability of its F-BAR domain to deform membranes and form filopodia-like membrane protrusions. This is a surprising finding since F-BAR domains have been mostly characterized for their ability to induce membrane tubulation and invaginations (Frost et al., 2008; Habermann, 2004; Henne et al., 2007; Itoh and De Camilli, 2006; Peter et al., 2004; Shimada et al., 2007). F-BAR domains are composed of a series of α helices forming a strong dimerization motif, which allow the homodimers to adopt a quaternary "banana-like" structure (Frost et al., 2008; Henne et al., 2007; Peter et al., 2004; Shimada et al., 2007). One possibility for how srGAP2's F-BAR domain may induce filopodia-like protrusions is by having a different curvature leading to a different surface distribution of positively charged residues than "canonical" F-BAR domains. Interestingly, I-BAR domains present in proteins such as

IRSp53 or MIM induce filopodia, a property linked to the inherent curvature of the I-BAR homodimer and the presence of phospholipid-binding residues on the convex side of the homodimers (Lim et al., 2008; Mattila et al., 2007; Millard et al., 2007; Saarikangas et al., 2009).

We hypothesize that the homodimer formed by the F-BAR domain of srGAP2 displays a general quaternary structure and charge distribution comparable to I-BAR domains. While this can only be proven by structural information, we provide several lines of evidence supporting an I-BAR like behavior: (a) the structural maintenance of filopodia induced by the F-BAR domain of srGAP2 is resistant to F-actin depolymerization, (b) overexpression of the F-BAR domain of srGAP2 does not inhibit endocytosis, and (c) the F-BAR domain of srGAP2 induces similar liposome deformations compared to IRSp53 (Suetsugu et al., 2006).

Interestingly, srGAP2 is not the only predicted F-BAR domain-containing protein inducing filopodia formation: Gas7 and PSTPIP2 (MAYP) have also been shown to induce filopodia in cell lines (Chitu et al., 2005; She et al., 2002). However, these proteins and more importantly their predicted F-BAR domains have not been directly tested for their ability to deform membranes. Our results suggest that the F-BAR domain subfamily could be functionally diverse and that this diversity might be due to subtle structural differences.

A Role for srGAP2 during Neuronal Development

It was recently shown that filopodia were required for neurite initiation in cortical neurons (Dent et al., 2007). The absence of effect of srGAP2 knockdown on neurite initiation is likely due to the presence of many other proteins involved in filopodia formation such as I-BAR-containing proteins such as IRSp53 or ABBA (Mattila and Lappalainen, 2008; Saarikangas et al., 2008) or other classes of proteins previously shown to promote filopodia formation and neurite initiation through distinct mechanisms (Dent et al., 2007; Kwiatkowski et al., 2007).

The ability of srGAP2 to promote neurite initiation and branching appears to also be important for its regulation of migration (Figure 7H). Knockdown of srGAP2 increased the rate of migration and significantly reduced LP complexity and branching (Figure 7H). This could potentially explain the increase in the rate of cell migration, since in fibroblasts, reduction of the activity of proteins promoting filopodia formation, such as ENA/VASP proteins, increased lamellipodia persistence and increased cell speed (Bear et al., 2000, 2002). In addition, it was recently shown that loss of ENA/VASP proteins in cortical neurons lead to a more superficial laminar position, which could be due to increased rate of migration (Goh et al., 2002; Kwiatkowski et al., 2007). Recent siRNA screens in cancer cell lines revealed that downregulation of the srGAP2 homologue srGAP3 also increased the rate of cell migration, suggesting that negative regulation of cell migration may be a conserved function of the srGAP family (Simpson et al., 2008).

Regulation of srGAP2: GAP and SH3 Domains

The BAR superfamily of proteins are involved in a wide range of functions and this diversity arises from the different functional domains associated with BAR-like domain (Itoh and De Camilli, 2006). We demonstrate that srGAP2 is a Rac1-specific GAP (as previously shown for srGAP3) and recent work has highlighted the importance of Rac1 regulation in neuronal development (Govek et al., 2005). Mutation of the Rac1/Cdc42 GEF ARHGEF6 (also called Cool-2 or α-PIX) results in X-linked mental retardation, suggesting the importance of properly regulating Rac1 activity during neuronal development (Kutsche et al., 2000). Interestingly, the BAR domain-containing protein Oligophrenin-1 as well as the F-BAR-containing protein srGAP3 (also called mental retardation GAP or MEGAP) are both Rac1-GAPs that have been involved in severe forms of mental retardation (Billuart et al., 1998; Endris et al., 2002; Govek et al., 2004).

Rac1 has also been implicated in regulating radial migration and neurite outgrowth (Causeret et al., 2008; Govek et al., 2005; Kawauchi et al., 2003; Konno et al., 2005; Yoshizawa et al., 2005). Although not required, the GAP activity of srGAP2 might play a role in neurite formation in two ways: (1) local inactivation of Rac1 could result in increased Cdc42 activity, which could in turn activate pathways that promote bundled F-actin that are required for filopodia formation (Raftopoulou and Hall, 2004), and/or, (2) alternatively, Rac1 inactivation could lead to increased activation of RhoA (since Rac1 activation has been shown to inactivate RhoA [Nimnual et al., 2003]), which in turn could lead to the activation of the formin mDia2 and increased actin nucleation (Figure 7G).

A high percentage of F-BAR domain-containing proteins possess SH3 domains (Itoh and De Camilli, 2006), which bind to effectors ranging from regulators of endocytosis such as dynamin (Itoh and De Camilli, 2006) to regulators of actin polymerization (Aspenstrom et al., 2006; Chitu et al., 2005) such as WAVE1 (Soderling et al., 2002). The SH3 domain of srGAP2 has been shown to bind the Robo1 receptor (Wong et al., 2001) and has also been shown to bind N-WASP (Linkermann et al., 2009), but the functional relevance of these interactions has yet to be determined. Our results strongly suggest that srGAP2 is autoinhibited at resting state, which is a commonly accepted model of regulation of many RhoGEF and RhoGAP proteins (Rossman et al., 2005) and the BAR domain-containing proteins GRAF and Oligophrenin-1 (Eberth et al., 2009). Future experiments will test if this autoinhibition can be released by effector binding to the SH3 domain exposing the F-BAR domain to facilitate membrane protrusion (Figure 7G).

EXPERIMENTAL PROCEDURES

Animals

Mice were used according to a protocol approved by the Institutional Animal Care and Use Committee at the University of North Carolina-Chapel Hill and in accordance with National Institutes of Health guidelines. Time-pregnant females were maintained in a 12 hr light/dark cycle and obtained by overnight breeding with males of the same strain. Noon following breeding is considered as E0.5.

Protein Purification

srGAP2 (amino acids 1–785) and F-BAR (amino acids 22–501) were cloned into pLIC vectors and expressed in *Escherichia coli* BL21 (DE3) cells. Proteins were then purified on a Ni2+ affinity column. Proteins were further purified by cation exchange chromatography, using a Source S column, and concentrated in 20 mM Tris buffer (pH 8), 150 mM NaCl, 1 mM DTT, and 5% glycerol. GAP (amino acids 502–676) and GAP^{R527L} domain of srGAP2 was cloned into pGex-4T3 (Amersham). Recombinant GST fusion proteins were then purified

using glutathione sepharose and resuspended in 20 mM Tris buffer (pH 8), 150 mM NaCl, 1 mM DTT, and 5% glycerol.

In Vitro GAP Assay

In vitro fluorescent-based GAP assay was performed as described previously (Shutes and Der, 2006).

Liposome Preparation, Liposome Tubulation Assays, and Electron Microscopy

Folch Fraction I Brain Lipid Extract from bovine brain (B1502) in chloroform was obtained from Sigma-Aldrich and used without further purification (see Supplemental Experimental Procedures for details; Itoh et al., 2005). The liposomes described above were first subjected to ten cycles of freeze-thaw, and then used immediately or stored in aliquots at −80°C. The liposomes were then equilibrated at RT for 1 hr before adding protein (either FBP17 F-BAR domain or srGAP2 F-BAR) at a lipid/protein ratio of 2:1 mass/mass and final concentrations of 0.2 mg/ml (lipid) and 0.1 mg/ml (protein). The tubulation reaction incubated for 30 min at room temperature before negative staining, as described below. In order to introduce the recombinant purified F-BAR into the liposomes, 250 μl of the tubulation reaction was subjected to 5 s of bath sonication at room temperature immediately after adding protein. After sonication, the sample was allowed to incubate for another 30 min before negative staining and processed for electron microscopy as described in the Supplemental Experimental Procedures (see also Frost et al., 2008).

Ex Vivo Cortical Electroporation and Primary Cortical Neuron Cultures

Mouse cortical progenitors were electroporated ex vivo at E15 as described previously (Hand et al., 2005). Following electroporation, cerebral hemispheres were either (1) dissected, enzymatically dissociated with papain, and plated on poly-L-lysine and Laminin-coated glass coverslips as described previously (Polleux and Ghosh, 2002); or (2) sliced using a LEICA VT1000S vibratome and cultured organotypically as described previously (Hand et al., 2005; see Supplemental Experimental Procedures for details).

Sequence alignments, shRNA and cDNA constructs and neuronal cultures, and confocal microscopy are detailed in the Supplemental Experimental Procedures.

SUPPLEMENTAL DATA

Supplemental Data contain Supplemental Experimental Procedures, 14 figures, and 8 movies and can be found with this article online at http://www.cell.com/supplemental/S0092-8674(09)00794-6.

ACKNOWLEDGMENTS

We thank the members of the Polleux and Jim Bear laboratories for helpful comments. We thank Carol Schuurmans and Pierre Mattar for in situ hybridization and the original srGAP2 cDNA. We thank the Sondek (Rafael Rojas) and Der (Adam Shutes) laboratories for technical assistance with protein purification and fluorescent GTP hydrolysis assay. We thank Brenda Temple for technical assistance with protein modeling and sequence analysis. We thank Vinzenz Unger, Carsten Mim, and Pietro De Camilli for helpful discussions. This work was supported by a Predoctoral Research Training Fellowship from the Epilepsy Foundation (A.F.) and a National Institutes of Health (NIH) Medical Scientist Training Program award (TG 5T32GM07205 to A.F.), an NIH Predoctoral Fellowship (5F31NS052969-03 to S.G.), University of North Carolina Developmental Biology Training Grant (T32 HD046369 to J.C.B.), a Pew Scholar Award in Biomedical Sciences (F.P.), and the National Institute of Neurological Disorders and Stroke Institutional Center Core Grant to Support Neuroscience Research (P30 NS45892-01).

Received: October 16, 2008
Revised: March 19, 2009
Accepted: June 25, 2009
Published: September 3, 2009

REFERENCES

Aspenstrom, P., Fransson, A., and Richnau, N. (2006). Pombe Cdc15 homology proteins: regulators of membrane dynamics and the actin cytoskeleton. Trends Biochem. Sci. *31*, 670–679.

Ayala, R., Shu, T., and Tsai, L.H. (2007). Trekking across the brain: the journey of neuronal migration. Cell *128*, 29–43.

Bacon, C., Endris, V., and Rappold, G. (2009). Dynamic expression of the Slit-Robo GTPase activating protein genes during development of the murine nervous system. J. Comp. Neurol. *513*, 224–236.

Bear, J.E., Loureiro, J.J., Libova, I., Fassler, R., Wehland, J., and Gertler, F.B. (2000). Negative regulation of fibroblast motility by Ena/VASP proteins. Cell *101*, 717–728.

Bear, J.E., Svitkina, T.M., Krause, M., Schafer, D.A., Loureiro, J.J., Strasser, G.A., Maly, I.V., Chaga, O.Y., Cooper, J.A., Borisy, G.G., et al. (2002). Antagonism between Ena/VASP proteins and actin filament capping regulates fibroblast motility. Cell *109*, 509–521.

Billuart, P., Bienvenu, T., Ronce, N., des Portes, V., Vinet, M.C., Zemni, R., Roest Crollius, H., Carrie, A., Fauchereau, F., Cherry, M., et al. (1998). Oligophrenin-1 encodes a rhoGAP protein involved in X-linked mental retardation. Nature *392*, 923–926.

Burnette, D.T., Schaefer, A.W., Ji, L., Danuser, G., and Forscher, P. (2007). Filopodial actin bundles are not necessary for microtubule advance into the peripheral domain of Aplysia neuronal growth cones. Nat. Cell Biol. *9*, 1360–1369.

Causeret, F., Terao, M., Jacobs, T., Nishimura, Y.V., Yanagawa, Y., Obata, K., Hoshino, M., and Nikolic, M. (2008). The p21-activated kinase is required for neuronal migration in the cerebral cortex. Cereb. Cortex *19*, 861–875.

Chitu, V., Pixley, F.J., Macaluso, F., Larson, D.R., Condeelis, J., Yeung, Y.G., and Stanley, E.R. (2005). The PCH family member MAYP/PSTPIP2 directly regulates F-actin bundling and enhances filopodia formation and motility in macrophages. Mol. Biol. Cell *16*, 2947–2959.

Dent, E.W., Barnes, A.M., Tang, F., and Kalil, K. (2004). Netrin-1 and semaphorin 3A promote or inhibit cortical axon branching, respectively, by reorganization of the cytoskeleton. J. Neurosci. *24*, 3002–3012.

Dent, E.W., Kwiatkowski, A.V., Mebane, L.M., Philippar, U., Barzik, M., Rubinson, D.A., Gupton, S., Van Veen, J.E., Furman, C., Zhang, J., et al. (2007). Filopodia are required for cortical neurite initiation. Nat. Cell Biol. *9*, 1347–1359.

Doherty, G.J., and McMahon, H.T. (2008). Mediation, modulation, and consequences of membrane-cytoskeleton interactions. Annu. Rev. Biophys. *37*, 65–95.

Dotti, C.G., Sullivan, C.A., and Banker, G.A. (1988). The establishment of polarity by hippocampal neurons in culture. J. Neurosci. *8*, 1454–1468.

Eberth, A., Lundmark, R., Gremer, L., Dvorsky, R., Koessmeier, K.T., McMahon, H.T., and Ahmadian, M.R. (2009). A BAR domain-mediated autoinhibitory mechanism for RhoGAPs of the GRAF family. Biochem. J. *417*, 371–377.

Endris, V., Wogatzky, B., Leimer, U., Bartsch, D., Zatyka, M., Latif, F., Maher, E.R., Tariverdian, G., Kirsch, S., Karch, D., et al. (2002). The novel Rho-GTPase activating gene MEGAP/ srGAP3 has a putative role in severe mental retardation. Proc. Natl. Acad. Sci. USA *99*, 11754–11759.

Frost, A., Perera, R., Roux, A., Spasov, K., Destaing, O., Egelman, E.H., De Camilli, P., and Unger, V.M. (2008). Structural basis of membrane invagination by F-BAR domains. Cell *132*, 807–817.

Frost, A., Unger, V.M., and De Camilli, P. (2009). The BAR domain superfamily: membrane-molding macromolecules. Cell *137*, 191–196.

Gallo, G., and Letourneau, P.C. (1998). Localized sources of neurotrophins initiate axon collateral sprouting. J. Neurosci. *18*, 5403–5414.

Gallo, G., and Letourneau, P.C. (2004). Regulation of growth cone actin filaments by guidance cues. J. Neurobiol. *58*, 92–102.

Goh, K.L., Cai, L., Cepko, C.L., and Gertler, F.B. (2002). Ena/VASP proteins regulate cortical neuronal positioning. Curr. Biol. *12*, 565–569.

Govek, E.E., Newey, S.E., Akerman, C.J., Cross, J.R., Van der Veken, L., and Van Aelst, L. (2004). The X-linked mental retardation protein oligophrenin-1 is required for dendritic spine morphogenesis. Nat. Neurosci. *7*, 364–372.

Govek, E.E., Newey, S.E., and Van Aelst, L. (2005). The role of the Rho GTPases in neuronal development. Genes Dev. *19*, 1–49.

Gupta, A., Sanada, K., Miyamoto, D.T., Rovelstad, S., Nadarajah, B., Pearlman, A.L., Brunstrom, J., and Tsai, L.H. (2003). Layering defect in p35 deficiency is linked to improper neuronal-glial interaction in radial migration. Nat. Neurosci. *6*, 1284–1291.

Gupton, S.L., and Gertler, F.B. (2007). Filopodia: the fingers that do the walking. Sci. STKE *2007*, re5.

Habermann, B. (2004). The BAR-domain family of proteins: a case of bending and binding? EMBO Rep. *5*, 250–255.

Hand, R., Bortone, D., Mattar, P., Nguyen, L., Heng, J.I., Guerrier, S., Boutt, E., Peters, E., Barnes, A.P., Parras, C., et al. (2005). Phosphorylation of Neurogenin2 specifies the migration properties and the dendritic morphology of pyramidal neurons in the neocortex. Neuron *48*, 45–62.

Heng, J.I., Nguyen, L., Castro, D.S., Zimmer, C., Wildner, H., Armant, O., Skowronska-Krawczyk, D., Bedogni, F., Matter, J.M., Hevner, R., et al. (2008). Neurogenin 2 controls cortical neuron migration through regulation of Rnd2. Nature *455*, 114–118.

Henne, W.M., Kent, H.M., Ford, M.G., Hegde, B.G., Daumke, O., Butler, P.J., Mittal, R., Langen, R., Evans, P.R., and McMahon, H.T. (2007). Structure and analysis of FCHo2 F-BAR domain: a dimerizing and membrane recruitment module that effects membrane curvature. Structure *15*, 839–852.

Higginbotham, H.R., and Gleeson, J.G. (2007). The centrosome in neuronal development. Trends Neurosci. *30*, 276–283.

Itoh, T., and De Camilli, P. (2006). BAR, F-BAR (EFC) and ENTH/ANTH domains in the regulation of membrane-cytosol interfaces and membrane curvature. Biochim. Biophys. Acta *1761*, 897–912.

Itoh, T., Erdmann, K.S., Roux, A., Habermann, B., Werner, H., and De Camilli, P. (2005). Dynamin and the actin cytoskeleton cooperatively regulate plasma membrane invagination by BAR and F-BAR proteins. Dev. Cell *9*, 791–804.

Kakimoto, T., Katoh, H., and Negishi, M. (2006). Regulation of neuronal morphology by Toca-1, an F-BAR/EFC protein that induces plasma membrane invagination. J. Biol. Chem. *281*, 29042–29053.

Kawauchi, T., Chihama, K., Nabeshima, Y., and Hoshino, M. (2003). The in vivo roles of STEF/Tiam1, Rac1 and JNK in cortical neuronal migration. EMBO J. *22*, 4190–4201.

Konno, D., Yoshimura, S., Hori, K., Maruoka, H., and Sobue, K. (2005). Involvement of the phosphatidylinositol 3-kinase/rac1 and cdc42 pathways in radial migration of cortical neurons. J. Biol. Chem. *280*, 5082–5088.

Kutsche, K., Yntema, H., Brandt, A., Jantke, I., Nothwang, H.G., Orth, U., Boavida, M.G., David, D., Chelly, J., Fryns, J.P., et al. (2000). Mutations in ARHGEF6, encoding a guanine nucleotide exchange factor for Rho GTPases, in patients with X-linked mental retardation. Nat. Genet. *26*, 247–250.

Kwiatkowski, A.V., Rubinson, D.A., Dent, E.W., Edward van Veen, J., Leslie, J.D., Zhang, J., Mebane, L.M., Philippar, U., Pinheiro, E.M., Burds, A.A., et al. (2007). Ena/VASP Is Required for neuritogenesis in the developing cortex. Neuron *56*, 441–455.

Lambert de Rouvroit, C., and Goffinet, A.M. (2001). Neuronal migration. Mech. Dev. *105*, 47–56.

Li, X., Chen, Y., Liu, Y., Gao, J., Gao, F., Bartlam, M., Wu, J.Y., and Rao, Z. (2006). Structural basis of Robo proline-rich motif recognition by the srGAP1 Src homology 3 domain in the Slit-Robo signaling pathway. J. Biol. Chem. *281*, 28430–28437.

Lim, K.B., Bu, W., Goh, W.I., Koh, E., Ong, S.H., Pawson, T., Sudhaharan, T., and Ahmed, S. (2008). The Cdc42 effector IRSp53 generates filopodia by coupling membrane protrusion with actin dynamics. J. Biol. Chem. *283*, 20454–20472.

Linkermann, A., Gelhaus, C., Lettau, M., Qian, J., Kabelitz, D., and Janssen, O. (2009). Identification of interaction partners for individual SH3 domains of Fas ligand associated members of the PCH protein family in T lymphocytes. Biochim. Biophys. Acta *1794*, 168–176.

Luo, L. (2002). Actin cytoskeleton regulation in neuronal morphogenesis and structural plasticity. Annu. Rev. Cell Dev. Biol. *18*, 601–635.

Mattar, P., Britz, O., Johannes, C., Nieto, M., Ma, L., Rebeyka, A., Klenin, N., Polleux, F., Guillemot, F., and Schuurmans, C. (2004). A screen for downstream effectors of Neurogenin2 in the embryonic neocortex. Dev. Biol. *273*, 373–389.

Mattila, P.K., and Lappalainen, P. (2008). Filopodia: molecular architecture and cellular functions. Nat. Rev. Mol. Cell Biol. *9*, 446–454.

Mattila, P.K., Pykalainen, A., Saarikangas, J., Paavilainen, V.O., Vihinen, H., Jokitalo, E., and Lappalainen, P. (2007). Missing-in-metastasis and IRSp53 deform PI(4,5)P2-rich membranes by an inverse BAR domain-like mechanism. J. Cell Biol. *176*, 953–964.

Millard, T.H., Dawson, J., and Machesky, L.M. (2007). Characterisation of IRTKS, a novel IRSp53/MIM family actin regulator with distinct filament bundling properties. J. Cell Sci. *120*, 1663–1672.

Mitin, N., Betts, L., Yohe, M.E., Der, C.J., Sondek, J., and Rossman, K.L. (2007). Release of autoinhibition of ASEF by APC leads to CDC42 activation and tumor suppression. Nat. Struct. Mol. Biol. *14*, 814–823.

Nimnual, A.S., Taylor, L.J., and Bar-Sagi, D. (2003). Redox-dependent downregulation of Rho by Rac. Nat. Cell Biol. *5*, 236–241.

Noctor, S.C., Martinez-Cerdeno, V., Ivic, L., and Kriegstein, A.R. (2004). Cortical neurons arise in symmetric and asymmetric division zones and migrate through specific phases. Nat. Neurosci. *7*, 136–144.

Ohshima, T., Hirasawa, M., Tabata, H., Mutoh, T., Adachi, T., Suzuki, H., Saruta, K., Iwasato, T., Itohara, S., Hashimoto, M., et al. (2007). Cdk5 is required for multipolar-to-bipolar transition during radial neuronal migration and proper dendrite development of pyramidal neurons in the cerebral cortex. Development *134*, 2273–2282.

Peter, B.J., Kent, H.M., Mills, I.G., Vallis, Y., Butler, P.J., Evans, P.R., and McMahon, H.T. (2004). BAR domains as sensors of membrane curvature: the amphiphysin BAR structure. Science *303*, 495–499.

Polleux, F., and Ghosh, A. (2002). The slice overlay assay: a versatile tool to study the influence of extracellular signals on neuronal development. Sci. STKE *2002*, PL9.

Raftopoulou, M., and Hall, A. (2004). Cell migration: Rho GTPases lead the way. Dev. Biol. *265*, 23–32.

Rossman, K.L., Der, C.J., and Sondek, J. (2005). GEF means go: turning on RHO GTPases with guanine nucleotide-exchange factors. Nat. Rev. Mol. Cell Biol. *6*, 167–180.

Saarikangas, J., Hakanen, J., Mattila, P.K., Grumet, M., Salminen, M., and Lappalainen, P. (2008). ABBA regulates plasma-membrane and actin dynamics to promote radial glia extension. J. Cell Sci. *121*, 1444–1454.

Saarikangas, J., Zhao, H., Pykalainen, A., Laurinmaki, P., Mattila, P.K., Kinnunen, P.K., Butcher, S.J., and Lappalainen, P. (2009). Molecular mechanisms of membrane deformation by I-BAR domain proteins. Curr. Biol. *19*, 95–107.

Scita, G., Confalonieri, S., Lappalainen, P., and Suetsugu, S. (2008). IRSp53: crossing the road of membrane and actin dynamics in the formation of membrane protrusions. Trends Cell Biol. *18*, 52–60.

She, B.R., Liou, G.G., and Lin-Chao, S. (2002). Association of the growth-arrest-specific protein Gas7 with F-actin induces reorganization of microfilaments and promotes membrane outgrowth. Exp. Cell Res. *273*, 34–44.

Shimada, A., Niwa, H., Tsujita, K., Suetsugu, S., Nitta, K., Hanawa-Suetsugu, K., Akasaka, R., Nishino, Y., Toyama, M., Chen, L., et al. (2007). Curved EFC/F-BAR-domain dimers are joined end to end into a filament for membrane invagination in endocytosis. Cell *129*, 761–772.

Shutes, A., and Der, C.J. (2006). Real-time in vitro measurement of intrinsic and Ras GAP-mediated GTP hydrolysis. Methods Enzymol. *407*, 9–22.

Simpson, K.J., Selfors, L.M., Bui, J., Reynolds, A., Leake, D., Khvorova, A., and Brugge, J.S. (2008). Identification of genes that regulate epithelial cell migration using an siRNA screening approach. Nat. Cell Biol. *10*, 1027–1038.

Soderling, S.H., Binns, K.L., Wayman, G.A., Davee, S.M., Ong, S.H., Pawson, T., and Scott, J.D. (2002). The WRP component of the WAVE-1 complex attenuates Rac-mediated signalling. Nat. Cell Biol. *4*, 970–975.

Suetsugu, S., Murayama, K., Sakamoto, A., Hanawa-Suetsugu, K., Seto, A., Oikawa, T., Mishima, C., Shirouzu, M., Takenawa, T., and Yokoyama, S. (2006). The RAC binding domain/IRSp53-MIM homology domain of IRSp53 induces RAC-dependent membrane deformation. J. Biol. Chem. *281*, 35347–35358.

Tsujita, K., Suetsugu, S., Sasaki, N., Furutani, M., Oikawa, T., and Takenawa, T. (2006). Coordination between the actin cytoskeleton and membrane deformation by a novel membrane tubulation domain of PCH proteins is involved in endocytosis. J. Cell Biol. *172*, 269–279.

Wong, K., Ren, X.R., Huang, Y.Z., Xie, Y., Liu, G., Saito, H., Tang, H., Wen, L., Brady-Kalnay, S.M., Mei, L., et al. (2001). Signal transduction in neuronal migration: roles of GTPase activating proteins and the small GTPase Cdc42 in the Slit-Robo pathway. Cell *107*, 209–221.

Yao, Q., Jin, W.L., Wang, Y., and Ju, G. (2008). Regulated shuttling of Slit-Robo-GTPase activating proteins between nucleus and cytoplasm during brain development. Cell. Mol. Neurobiol. *28*, 205–221.

Yohe, M.E., Rossman, K.L., Gardner, O.S., Karnoub, A.E., Snyder, J.T., Gershburg, S., Graves, L.M., Der, C.J., and Sondek, J. (2007). Auto-inhibition of the Dbl family protein Tim by an N-terminal helical motif. J. Biol. Chem. *282*, 13813–13823.

Yoshizawa, M., Kawauchi, T., Sone, M., Nishimura, Y.V., Terao, M., Chihama, K., Nabeshima, Y., and Hoshino, M. (2005). Involvement of a Rac activator, P-Rex1, in neurotrophin-derived signaling and neuronal migration. J. Neurosci. *25*, 4406–4419.